THYROID
Volume 1, Number 3, 1991
Mary Ann Liebert, Inc., Publishers

Localization of Human Thyroxine Absorption

MARGUERITE T. HAYS

ABSTRACT

The distribution of intestinal absorption of ^{131}I-labeled thyroxine (T_4*) was studied in 4 normal subjects after oral and i.v. T_4*, given in separate experimental sessions. In addition to collection of time-activity curves for plasma T_4* from the two sessions, distribution and transport of T_4* through the gut was quantified by external imaging. Time–activity curves were obtained for the stomach, duodenum, and upper jejunoileum. A multicompartmental model for systemic T_4, with three distribution compartments and a single exit route, was employed. Additional, gastrointestinal, compartments were introduced. The stomach data were fitted to a model with three compartments, two for transport and a small sink of gastric activity that does not interact with the absorptive sites. Transfer from the duodenum to the upper jejunoileum and from the upper to the lower jejunoileum was modeled from fits to the peak T_4* activities in the images of the duodenum and upper jejunoileum. The rate of transfer from the lower jejunoileum into more distal intestinal sites was fixed, but the impact on the results of using various values for this parameter was analyzed. The model calculations of absorption (mean ± SD for 3 of the subjects) are duodenum, 15 ± 5%, upper jejunoileum, 29 ± 14%, and lower jejunoileum, 24 ± 11%. The fourth subject, whose global absorption was abnormally low for uncertain reasons, had 17% absorption from the duodenum, 9% from the upper jejunoileum and none from the lower jejunoileum. Model projections mimicking clinical gut abnormalities known to affect T_4 absorption were compatible with the results of published studies.

INTRODUCTION

ABSORPTION OF THYROXINE (T_4) INTO THE GENERAL CIRCULATION after oral administration is known to be incomplete and variable.[1] Factors affecting this absorption are incompletely understood, among them the locations in the intestine most important for T_4 absorption. This study, in normal human volunteers, was undertaken to identify the sites of T_4 absorption within the gut, using tracer imaging and mathematical modeling techniques together with analysis of plasma tracer appearance and disappearance curves.

MATERIALS AND METHODS

Tracer preparation

^{131}I T_4 (T_4*) was prepared by radioiodination of stable 3,5,3′-T_3 with ^{131}I iodide, using the chloramine-T method. This method of iodination yields T_4* that is essentially carrier-free. The T_4* fraction from HPLC purification was evaporated to remove organic solvents, reconstituted with human serum albumin (HSA) in normal saline solution to a final HSA concentration of 1% by weight, and then sterilized by Millipore filtration. Before i.v. administration, aliquots of the solution were tested for sterility and freedom from pyrogens.

For practical reasons, the actual volume of the T_4* solution given in the oral studies varied, and so the amount of HSA given with the oral dose also varied, from 20 mg to 167 mg (see Discussion).

Subjects and sessions

Five normal, consenting, paid volunteers, 2 men and 3 women, ages 26–59 years, each participated in two experimental sessions with ^{131}I-T_4 administration at an interval of 2 or more weeks, one with i.v. tracer, the other with oral tracer. Subjects received Lugol's solution (10 drops 30 min before

Department of Veterans Affairs Medical Center, Palo Alto, CA, and the Departments of Radiology, Medicine, and Surgery, University of California at Davis School of Medicine, Sacramento, California.

tracer injection, repeated every second day for 2 weeks) to suppress thyroidal uptake of radioiodide. Subjects also received i.v. ^{99m}Tc-labeled erythrocytes in a third session, from which plasma volumes were calculated.

In one study (subject 4), the i.v. data were unusable. Accommodation for these missing data is described below. Also, the computer file containing the external imaging data for subject 5's oral T_4* session was unusable. His plasma data were used in establishing the core T_4* model and in the global absorption fits, but his study was not included in the final analysis, which required the external imaging data to localize T_4* absorption.

Experimental plan

In each experimental session, the fasting subject reclined under a computerized gamma scintillation camera, which was positioned to give an anterior view of the lower thorax and upper abdomen. Separate cannulae were used for the i.v. injection and for blood sampling. The oral dose was given through a drinking straw, and the container was washed repeatedly with a total of 200 mL of water swallowed through the same straw. Scintillation camera images were obtained in 5-min frames continuously for the first hour after tracer administration and then at approximately 2 h, 6 h, and 24 h. Blood samples were obtained at several time points during the first hour and then at approximately 2, 4, 6, and 24 h.

In addition to the data incorporated in this study, time–activity curves of plasma after oral and i.v. ^{125}I-T_4 glucuronide, of hepatic ^{131}I activity, and of cardiac and hepatic ^{99m}Tc activity were acquired. These data are being analyzed and will be reported separately.

This study was approved by the local Institutional Review Board for human studies and by the local Radiation Human Use Committee.

Data analysis

External imaging. The gamma camera images from the oral study were examined sequentially, and the stomach, duodenum, upper jejunoileum, lower jejunoileum, cecum, and colon were identified (Fig. 1). Each was flagged as a region of interest, and the counts within that region in each frame were recorded to establish time–activity data sets. The time of an observation was assumed to be the midpoint of its 5-min frame. An area of abdominal background was flagged in a part of the image that is free of gut activity. The counts in this background area were subtracted from the counts in the gut region of interest after being corrected for area differences.

Time–activity curves for the stomach, duodenum, and upper jejunoileum were defined and later incorporated into the model fits. The stomach curves incorporated all of the activity in the stomach region of interest, after correction for attenuation and background activity. However, the duodenal and upper jejunoileal areas overlapped with other areas also containing radioactivity at the same time (Fig. 1). Since these two curves were to be used only to identify the peak time of tracer residence, the flagged areas were drawn so as to avoid overlap insofar as possible. Little of the tracer had progressed into the lower jejunoileum by the end of the first hour's continuous data collection, and subsequent imaging data were limited to single

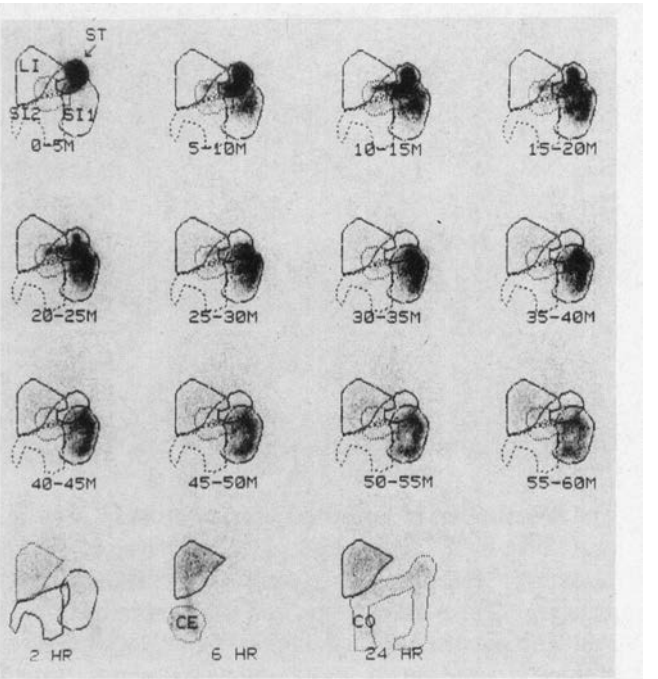

FIG. 1. External imaging data collection, subject 2. Each frame represents a 5-min data acquisition period. The areas identified from distribution of the radioactivity are indicated. ST, stomach; SI1, upper jejunoileum; SI2, lower jejunoileum; CE, cecum; CO, colon. The liver, LI, is indicated for orientation. The duodenal region, not labeled, is the looped area adjacent to the stomach and partially overlapping the liver. Data curves from the stomach, duodenum and upper jejunoileum in this study are presented in Figure 4.

images at 2, 6, and 24 h (Fig. 1). Hence, few observations were available reflecting the time periods when the tracer was primarily in the lower jejunoileum, cecum, or colon, and it was not possible to derive time–activity curves for these areas. Based on their appearance times, as well as on published estimates of small intestinal transport,[2,3] a 4 h mean residence time in the lower jejunoileum was assumed. Extrapolating from our own work in cats,[4] we assumed that T_4 absorption from the cecum and colon was not significant.

Plasma analysis. Aliquots of plasma samples were counted in a gamma counter together with a standard prepared from the administered dose. Total ^{131}I activity, as % dose/mL, was converted to % dose in the plasma volume by multiplying by the measured plasma volume.

Plasma samples were analyzed also on HPLC to determine the fraction of total radioactivity present as T_4. The values used in the model were the product of this fraction and the total % dose in the plasma volume. A control plasma sample spiked with the administered tracer was analyzed together with the experimental samples. The T_4* fraction in these spiked samples was 95 ± 15% of the oral and 95 ± 4% of the i.v. tracer. In analysis of the plasma samples obtained at 24 h, the T_4* fractions were 88 ± 5% and 94 ± 18% of total activity, respectively, for the oral and i.v. studies.

In setting up the model solutions, the time–activity curve for T_4* in the plasma volume was taken as the content of the central

(plasma) compartment. The percent present as T_4 in the spiked sample was used as the initial condition for the T_4* content of that compartment.

Modeling strategy

Technique. Mathematical modeling was done with the SAAM 30 program.[5,6]

The core T_4 and global absorption models* (Fig. 2). The plasma data from the i.v. study were fitted to a three-compartment mammillary model (Fig. 2a), as well established for such data.[7] To improve identifiability, only one exit route, from the fast-exchange compartment, was assumed. This simplifying assumption was considered to be acceptable, since the goal of this study does not require identification of the sites of T_4 metabolism and degradation. The same assumption was used in each of the model forms studied. Certainly, elimination of T_4 does occur from the slow-exchange compartment, but its inclusion would not be expected to affect the absorption rate or absorption fraction, the goals of the present study. Identifiability issues are discussed further below.

Once parameters for T_4 exchange and metabolism were established from fit of the i.v. data, the data from the oral study were fitted to a similar model, which, in addition, also incorporated a single compartment for the intestinal absorption site and a delay compartment proximal to the absorption site (Fig. 2b). Initially, only the length of the delay and the rates of absorption and loss from the absorptive sites (DT_9, $k_{12,7}$, and $k_{0,7}$) were fitted, holding the parameters for T_4 exchange and loss constant at the values derived from fitting the i.v. data. After the best possible fit was achieved with this restriction, the i.v. and oral data sets were fitted simultaneously, allowing all parameters to adjust.

The model in Figure 2b and also that shown in Figure 3 assume that absorption is into the fast-exchange compartment.

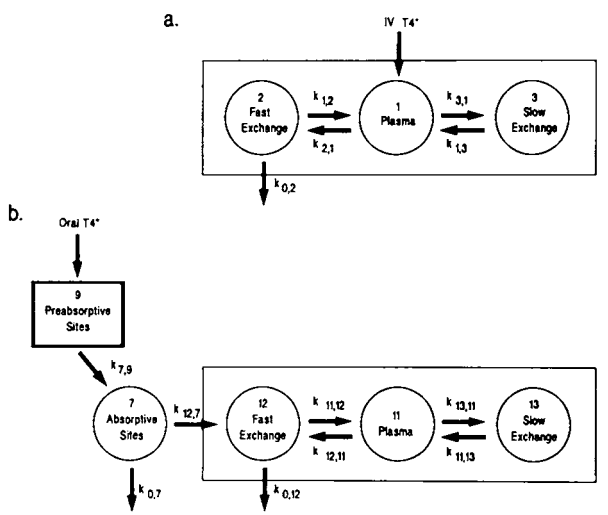

FIG. 2. The models used in the initial fits of the plasma time–activity curves to obtain global absorption values and to establish the core T_4* model. **a**. The model for fit of the data from the i.v. T_4* study. **b**. The model for fit of the data from the oral T_4* study.

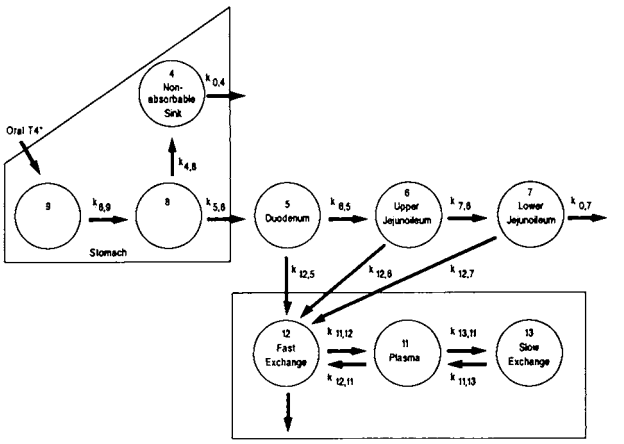

FIG. 3. The model used to establish the distribution of T_4* absorption. The stomach model (box on left) was fitted to the data from the stomach flags. The core T_4* model (box on right) was fixed with the parameters established from the fits of the models shown in Figure 1. Intestinal transport parameters $k_{6,5}$ and $k_{7,6}$ were established by visual comparison with data from flags of the duodenum and upper jejunoileum. The three parameters for absorption from the small intestine into the core T_4* model were then fitted to the observed data set for compartment 11. This model incorporates simplifying assumptions that are detailed in the Discussion.

This assumption is based on the belief that almost all of absorbed T_4 is delivered to the liver, a fast-exchange organ, through the portal circulation.

Finally, the eight data sets from the 4 subjects with complete plasma data sets for both the i.v. and the oral studies (subjects 1, 2, 3, and 5) were fitted simultaneously, limiting $k_{2,1}$ and $k_{3,1}$ so that their values were the same for all subjects but allowing them, as well as the other individual parameters, to adjust. This final smoothed fit was achieved without deterioration in the sums of squares for the fit to the data.

The plasma data from the oral T_4 session of subject 4, the subject without usable i.v. data, were then fitted to the geometric mean parameters of the smoothed model from the other 4 subjects. Only DT_9 and $k_{0,7}$ were adjusted in this fit, and the sum of squares of the fit of compartment 11 (plasma T_4* after oral administration) was similar to that of the other subjects.

These fits of the data to the simple model in Figure 2 yielded a global T_4 absorption value,[8] calculated from $k_{12,7}/(k_{12,7} + k_{0,7})$, which was used only for comparative purposes and not incorporated into the final analysis to localize T_4* absorption. These fits also yielded, for each subject, final adjusted parameters describing T_4 central kinetics. These core T_4* parameters were fixed in the subsequent modeling to define the T_4 absorptive sites.

Gastrointestinal kinetics. Data from the external imaging of gastric radioactivity were fitted to the stomach portion of the model shown in Figure 3. In order to fit the late stomach data, a very slow compartment (compartment 4) was required. Initially, compartment 4 was assumed to empty into the absorptive sites of the intestine, but this caused a major deterioration of fits of the late data. For that reason, in the final model (Fig. 3) compart-

ment 4 is a sink that removes T_4 from the absorptive pool. After an initial set of fits of the stomach data to this model, the model was simplified by fixing $k_{5,8}$ to the geometric mean of the original fits and then refitting the stomach data, adjusting only $k_{8,9}$ and $k_{4,8}$. After this refitting, the stomach parameters for each subject were fixed and incorporated into the final model.

Model fits to the data curves for the duodenum (compartment 5 in Figs. 3 and 4) and upper jejunoileum (compartment 6) were then approximated by adjusting their input and output parameters in the model to achieve calculated curves with activity peaks that visually matched the peaks of the data curves. These parameters were later readjusted further in tandem with the iterative fitting of the absorption parameters.

Localization of absorptive sites. Partition of T_4 absorption among the duodenum, the upper jejunoileum, and the lower jejunoileum was estimated by fitting the plasma T_4 data after oral administration (compartment 11) to the model shown in Figure 3. This model assumes that no absorption occurs at the cecum or below, so that physical transport from the lower jejunoileum ($k_{0,7}$) is considered to be an exit parameter for purposes of estimating T_4 absorption. This parameter was fixed at .00417/min, which corresponds to a mean physical residence time of unabsorbed bowel contents in the lower jejunoileum of 240 min. (Implications of this assumption are discussed later.) The parameters fitted in the final solution of the Figure 3 model were those for absorption from the duodenum, upper jejunoileum, and lower jejunoileum, $k_{12,5}$, $k_{12,6}$, and $k_{12,7}$, respectively, and those for transport down the gut from the duodenum and the upper jejunoileum, $k_{6,5}$ and $k_{7,6}$. Data for compartment 11 were fitted to the absorption parameters by iteration. The parameters for small intestinal transport, $k_{6,5}$ and $k_{7,6}$, were adjusted to the data curves for compartments 5 and 6 after each such iteration as described, and then the iteration was repeated. In these fits, the primary attention was to timing of the transit peaks rather than to measured compartment content, which was contaminated by radioactive crosstalk from nearby structures.

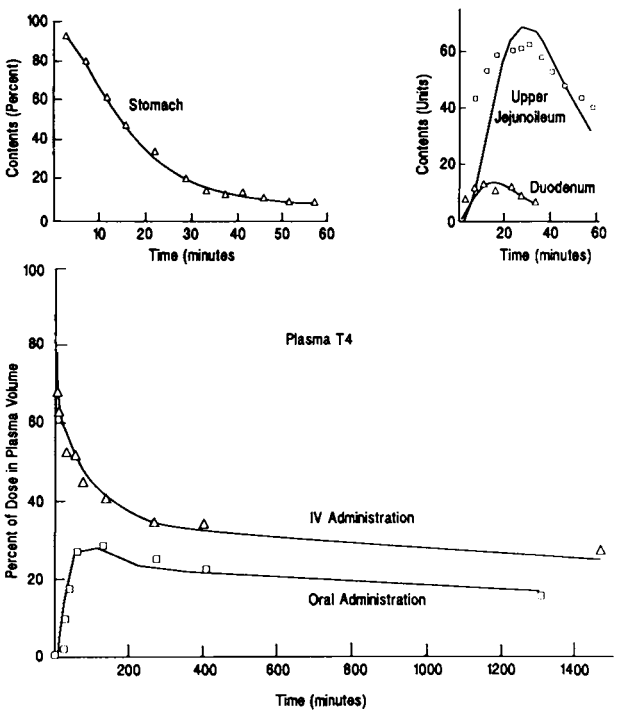

FIG. 4. Fit the model shown in Figure 3 to the data from subject 2, the same subject whose scintillation camera study is shown in Figure 1. Discrete points represent the observed counts in the flagged areas of external images of the stomach (top left) and the upper jejunoileum and duodenum (top right). The points in the lower panel represent the total plasma T_4* content. The solid lines show the values calculated from solution of the model.

RESULTS

Plasma volumes

Plasma volumes calculated from the distribution of ^{99m}Tc-labeled erythrocytes were 3593, 2422, 2188, 2287, and 3136 mL, respectively for subjects 1, 2, 3, 4, and 5.

The core T_4 model (Figs. 2 and 3, right lower segment)*

Rate constants for the plasma exchange model and global absorption model from Figure 2 are presented in Table 1. The mean fractional standard deviations (FSDs) of these parameters (a measure of the confidence of the parameter estimate) were $k_{2,1}$:0.27; $k_{1,2}$:0.37; $k_{3,1}$:0.16; $k_{1,3}$:0.43; $k_{0,2}$:0.91; DT_9:0.12; $k_{5,7}$:0.16; and $k_{0,7}$:0.32.

Global estimate of T_4 absorption*

Global absorption values derived from simultaneous solutions of the pairs of oral and i.v. data, using the models shown in Figure 2, are presented in Table 2 for the 4 subjects for whom abdominal imaging data were available. The other subject (subject 5) had a global absorption value of 75%.

Gastrointestinal transport parameters (Fig. 3)

Transport of the oral T_4 dose through the upper gastrointestinal tract, as determined by the imaging data, varied widely among the four subjects (Tables 1 and 2). The stomach parameters, $k_{8,9}$, $k_{5,8}$, and $k_{4,8}$, were derived as described previously. An example of such a fit of the stomach model to a data set is shown in the upper left segment of Figure 4.

In two cases, fit of the stomach data was improved by introduction of an additional, delay, compartment into the model, but the simpler model form shown was eventually accepted, since the purpose of modeling the stomach data was to provide an appropriate input function for the intestinal T_4 absorptive sites, and the more complex model could not be justified by the data available.

In the original fits of the model, a slow return from the stomach sink, compartment 4, was included. However, the data are insufficient to define the rate of this return, if it occurs, and its introduction led to poor late fits of the plasma data. For these reasons, compartment 4 is considered here to be only a sink,

TABLE 1. PARAMETERS OF THE FINAL DATA FITS TO MODELS SHOWN IN FIGURES 2 AND 3

	Subject					
	1	*2*	*3*	*4*	*5*	*Mean ± SD*
Core T_4* model parameters						
$k_{2,1} = k_{12,11}$	0.166	0.166	0.166	0.166[a]	0.166	0.166[b]
$k_{1,2} = k_{11,12}$	0.321	0.432	0.623	0.394[a]	0.159	0.384 ± 0.195
$k_{3,1} = k_{13,11}$	0.0076	0.0076	0.0076	0.0076[a]	0.0076	0.0076[b]
$k_{1,3} = k_{11,13}$	0.0042	0.0054	0.0046	0.0045[a]	0.0037	0.0045 ± 0.0007
$k_{0,2} = k_{0,12}$	0.0015	0.0017	0.0012	0.0013[a]	0.0006	0.0013 ± 0.0004
Global absorption parameters						
DT_9 (min)	7.3	4.6	15.8	8.2	32.4	13.7 ± 11.3
$k_{12,7}$	0.0122	0.0087	0.0077	0.0098	0.0113	0.0099 ± .0018
$k_{0,7}$	0.0323	0.0042	0.0028	0.0040	0.0040	0.0095 ± .0127
Transit parameters						
$k_{8,9}$	10.000	0.130	0.017	0.120		2.57 ± 4.96
$k_{4,8}$	0.001	0.010	0.020	0.025		0.014 ± 0.011
$k_{5,8}$	0.10	0.10	0.10	0.10		0.10[c]
$k_{6,5}$	0.10	0.14	0.20	0.10		0.14 ± 0.05
$k_{7,6}$	0.022	0.025	0.036	0.040		0.031 ± 0.009
$k_{0,7}$	0.0042	0.0042	0.0042	0.0042		0.0042[d]
Absorption parameters						
$k_{12,5}$	0.022	0.015	0.055	0.030		0.031 ± 0.017
$k_{12,6}$	0.003	0.028	0.039	0.011		0.020 ± 0.016
$k_{12,7}$	0.000	0.003	0.010	0.014		0.007 ± 0.006

[a]Subject 4's core model parameters were assumed to equal the geometric means of the other 4 subjects' values (see text).
[b]In the final combined solution of the core T_4* model, these parameters were constrained to be equal for all subjects.
[c]In the final fits of the stomach data, $k_{5,8}$ was fixed to the mean of its values derived from preliminary fits.
[d]$k_{0,7}$ is derived from an assumed 240 min MRT in the lower jejunoileum (see text).

representing alteration of a small part of the T_4 oral dose into a nonabsorbable form by the stomach itself or by its contents. (As discussed later, this assumption may be only partially valid.)

Fitting of the data from the areas of interest over the duodenum and upper jejunoileum were approximated as described previously. An example is in the upper right segment of Figure 4. Despite efforts to subtract out background and to avoid irrelevant areas of radioactivity in defining these areas, the data curves have uncertain limits. In fitting these data, the goal was limited to matching the location of the peaks of the curves, which were apparent from inspection. These provide the transport information required.

TABLE 2. GASTROINTESTINAL TRANSPORT AND ABSORPTION PARAMETERS

	Subject				*All*	*Omitting subject 1*	
	1	*2*	*3*	*4*	*Mean ± SD*	*Mean ± SD*	*Geometric mean*
From solution of Figure 2 models							
Mean residence times (min)							
Stomach	10	17	69	18	28 ± 27	35 ± 30	28
Duodenum	10	7	5	10	8 ± 2	7 ± 3	7
Upper jejunoileum	45	40	28	25	35 ± 10	31 ± 8	30
Lower jejunoileum (assumed)	240	240	240	240	240	240	240
T_4 absorption (%)							
Duodenum	17	9	17	18	15 ± 5	15 ± 5	14
Upper jejunoileum	9	42	32	14	24 ± 15	29 ± 14	26
Lower jejunoileum	0	15	21	37	18 ± 15	24 ± 11	23
Total T_4 absorption	26	65	70	69	58 ± 21	68 ± 3	68
T_4 lost in compartment 4 (%)	1	9	16	16	10 ± 7	14 ± 4	13
From solution of Figure 1 models							
Total T_4 absorption (%)	27	68	74	71	60 ± 22	71 ± 3	71
Albumin content of oral dose (mg)	167	45	40	97	87 ± 59	61 ± 32	56

Localization of intestinal absorption of T_4 (Fig. 3 model)

The calculated values for the absorption parameters, $k_{12,6}$, $k_{12,7}$, and $k_{12,8}$, are listed in Table 1. Mean FSDs were $k_{12,6}$:0.11; $k_{12,7}$:0.14; and $k_{12,8}$:0.11. The distribution of T_4 absorption between the duodenum, the upper jejunoileum, and the lower jejunoileum calculated from the intestinal transport and absorption parameters is presented in Table 2. Subject 1, the subject with reduced global absorption, had normal duodenal absorption but reduced absorption in the jejunoileum. The other 3 subjects showed distributed absorption throughout the small intestine.

Table 2 also demonstrates that a model solution using the full model (Fig. 3) yields a total absorption percent that is somewhat lower in each case than the global absorption calculated from the simple model (Fig. 2), which uses only the plasma data. This suggests that the sink in compartment 4 is overestimated. However, the fit of the two models to the plasma data after oral T_4 administration was comparable, so it is also possible that the simple model leads to a slight overestimate of T_4 absorption.

Projections of clinical situations

Using the geometric mean parameter values from subjects 2, 3, and 4, those who had normal T_4 absorption, the model was solved with various structural changes intended to mimic clinical situations that have been shown to affect T_4 absorption. Figure 5 shows the results of these projections. Bypass of the gastric antrum and duodenum, as in a Billroth II gastrectomy, was modeled by presenting the dose directly into compartment 6, the upper jejunoileum. Clinical studies have shown that the Billroth II procedure is associated with a modest increase in absorption fraction.[1] From the projection shown in Figure 5, it would appear that this is because of the bypass of compartment 4, the stomach sink. Bypassing of the duodenum in itself had almost no effect (not shown) presumably because of efficient absorption by the jejunoileum.

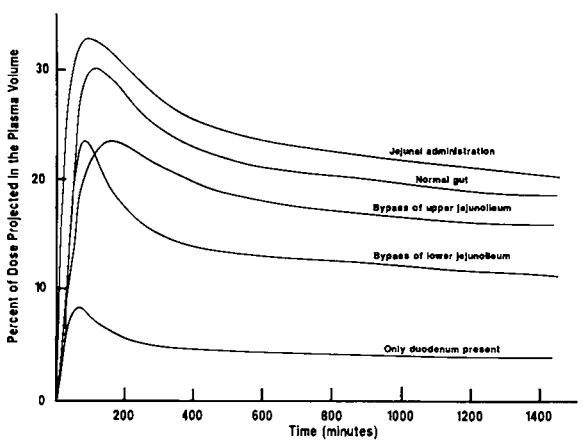

FIG. 5. Projections of time–activity curves for plasma T_4 after oral administration, using the model shown in Figure 3 with the geometric mean of the parameters for subjects 2, 3, and 4. The model was altered in each case to mimic the clinical situation indicated.

Bypass or absence of the upper jejunoileum, with an intact lower jejunoileum, was modeled by making the transport from compartment 6 to compartment 7 very rapid. For absence of distal bowel segments (the lower jejunoileum or the entire jejunoileum), the absorption parameters from the absent compartments were set to zero. Isolated bypass of the upper jejunoileum had a smaller overall effect than did isolated bypass of the lower jejunoileum, reflecting the fact that mean residence time in the upper jejunoileum is only 14% of that in the lower jejunoileum. When only the duodenum is present, projected absorption is very low.

DISCUSSION

Problems of model identifiability

The mathematical model employed is quite complex, and this complexity introduces questions of identifiability. The core T_4 model after i.v. administration, in the form used, with only one exit pathway, is, in principle, identifiable.[9,10] Although this simplified form is physiologically incorrect as a model for T_4 kinetics,[7] potential exit pathways from compartments 2 and 3 cannot be distinguished with the data available. For simplicity, the single exit model was chosen, and it was used in all of the comparative analyses. We have also introduced the simplifying assumption that the intrinsic T_4 model is the same, for a given subject, for oral and i.v. T_4*, even though they were studied in different sessions. With these assumptions, only three parameters still need to be adjusted in the global fit of the oral plasma curve (Fig. 2b), and this model is also identifiable. To make the intrinsic T_4 model as appropriate as possible for both of a subject's sessions, the data from both sessions were then fitted to equalized parameters. Presumably, this compromise fit is still identifiable.

Even though the intrinsic T_4 model is theoretically identifiable, the FSDs for fit of $k_{0,2}$ was unacceptably large (up to 3), probably because of data noise and suboptimal timing of samples.[11] These studies were terminated at 24 h, before full T_4* distribution had occurred, making separation of system exit from distribution difficult. As all of the subjects were euthyroid and none had any evidence of unusual intrinsic T_4 kinetics, the T_4 model for final application in the localization studies was further limited by solving the eight data sets from 4 subjects simultaneously, setting the parameters for exit from the plasma into each of the two peripheral compartments equal among the subjects but adjustable and allowing the other parameters to adjust freely for each subject. This led to greater comparability of the entire parameter set and caused no deterioration in the sum of squares of the fit of the various data sets to the model, compared to the separate individual fits.

It was possible to fit the data for the stomach time–activity curves to a variety of model forms, but most of them were clearly not identifiable. Since the purpose of modeling the stomach activity was simply to provide a proper input function for the duodenum and to quantify the nonabsorbed sink, a restricted model was used in the final analysis. With this model, in which $k_{5,8}$ was held constant, only two parameters were adjusted.

Once the intrinsic T_4 kinetics and the stomach input function were established, the transport parameters for the upper small

intestine are identifiable, there being only two parameters to fit to the two data sets, the time–activity curves for the duodenum and upper jejunoileum. [In truth, these fits are approximations only (Fig. 4) because of data problems, as discussed previously.] Once that is done, we are left with the three absorption parameters to fit to the oral sessions's T_4 time–activity curve. To assess the uniqueness of the absorption parameters arrived at by the original model fitting process, a form of sensitivity analysis was done. Attempts were made to force different sets of parameters to fit by fixing and adjusting one or another of the three absorption parameters and then iterating on the others. These maneuvers led to deterioration in the sum of squares of the model fit to the data, so it appears that the different absorption parameters provide separate information, though they are probably not separately identifiable in the technical sense.

Simplifying assumptions

Four important simplifying assumptions were used in this study. The first is that compartment 4 is assumed to be a simple sink. Since the total T_4 absorption calculated using the model in Figure 3 was slightly less than that using the global absorption model of Figure 2, it is likely that a portion of compartment 4 does eventually enter the absorption-available pool. However, this could not be sorted out using the data at hand, and employment of a model form in which compartment 4 *all* entered the absorption-available pool led to unacceptable deterioration in the model fits to the plasma data.

The second assumption is that the only disposal of T_4* in the small intestine is by absorption or transfer to a more distal site. This assumption is intrinsic to the assumption that the external images represent T_4* alone. Any metabolism of T_4* that which might occur proximal to an absorption site would lead to an overestimate of the T_4* available at that site and hence to an underestimate of its absorption.

The third assumption is that the mean residence time in the lower jejunoileum, compartment 7, is 4 h. To appraise the impact of this assumption, the model was refitted to the data from each of the 4 subjects using a series of assumed values for this time, ranging from 1.5 h to 6 h. In these fits, it was not necessary to adjust $k_{6,5}$ or $k_{7,6}$, since the shapes of the fits to compartments 5 and 6 were not affected by changes in the mean residence time in compartment 7. The fractional absorptions from the three intestinal compartments were unchanged in subject 1, the subject with no measurable absorption from compartment 7. The mean effects of the assumed compartment 7 mean residence time on the distribution of absorption in the other 3 subjects is presented in Figure 6. As mean residence time in compartment 7 increases, relatively more of the absorption is seen to be from the upper jejunoileum and relatively less from the lower jejunoileum and the duodenum. In 2 of the subjects, the sum of squares of the deviation from model fit was improved by shortening the mean residence time. In the third, it was improved by lengthening it. Fractional standard deviations among the 3 subjects were smaller with longer than with shorter mean residence times. This analysis is consistent with the assumption that a 4-h mean residence time in compartment 7 is reasonable.

The fourth assumption is that there is no T_4* absorption from the large intestine. This assumption is based on our own work

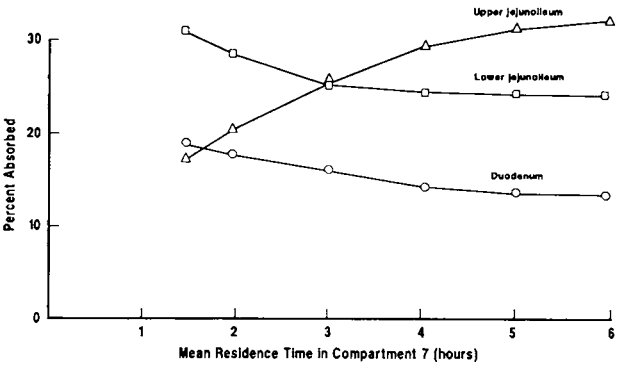

FIG. 6. Effect of the assumed mean residence time in compartment 7, the lower jejunoileum, on the calculated distribution of T_4 absorption. The model shown in Figure 3 was solved using the geometric means of the parameters from the solutions of subjects 2, 3, and 4. All parameters were fixed except the absorption parameters, $k_{12,5}$, $k_{12,6}$, and $k_{12,7}$. Different values for $k_{0,7}$, representing the mean residence times investigated, were also entered into the model as fixed parameters. The percent absorbed from each compartment was calculated as the percent of the dose entering that compartment times the ratio of the absorption rate from that compartment to its total exit.

demonstrating minimal absorption of T_4* instilled into the feline cecum.[4] It is supported by the human study reported by Stone et al.[12] showing no T_4* absorption in a patient with absent jejunum and ileum.

Variability in absorption fraction

In this study, the HSA content of the oral T_4 dose was not held constant. Tracers were made up to a constant HSA concentration, but varying dose volumes led to varying total protein content of the orally administered tracer (Table 2). Previous work has shown that a 10 mg HSA dose content does not retard T_4 absorption, whereas a 310 mg HSA dose content has a markedly retarding effect.[8] Subject 1, whose dose contained 157 mg HSA, had a global T_4 absorption (27%) that was even lower than that seen in a group of 10 normal subjects given 310 mg HSA with their T_4 tracer (47 ± 6%).[8] Global absorption values for the other 3 subjects with available gut transport data are within the normal range for a T_4 tracer dose given with 10 mg HSA (71 ± 9%). Subject 5, whose data are omitted from Table 2 because his gut transport imaging data were unusable, had 20 mg HSA in his oral T_4 dose and a normal global T_4 absorption of 75%. Other than the protein content of the dose, there is no apparent explanation for the unusually low T_4 absorption observed in subject 1.

Implications for human disease

T_4 absorption has been shown to be incomplete in the human and in all of the animal species in which it has been studied. A wide variety of factors are known to affect absorption, the most important among them being aberrations in the small intestine.[1] Results of this study show that absorption occurs all along the human small intestine, but the rapidity of absorption

appears to decrease as the dose proceeds distally. This slowing of absorption rate is balanced by the longer residence time in the lower small bowel. Hence, bypass of the duodenum causes little decrease in overall absorption despite the fact that the intrinsic absorption rate from the duodenum appears to be greater than is that in the lower small bowel. In fact, in our simulation study, instillation of the dose directly into the jejunum caused a mean increase in overall absorption efficiency because of bypassing of the gastric sink. This finding is consistent with the increased T_4* absorption observed in patients who have had Billroth II surgery.[1] Bypass of portions of the jejunoileum reduces T_4* absorption. These findings are in keeping with clinical reports of marked T_4 malabsorption after jejunoileal bypass surgery,[13–15] in patients with bowel resections,[12] and in those with mucosal diseases of the small bowel.[1]

ACKNOWLEDGMENTS

The author is grateful to Ms. Lichi Hsu for expert technical assistance. The staff of the Nuclear Medicine Service at the Palo Alto DVA Medical Center were of enormous assistance in carrying out this study. The author is especially indebted to Drs. David Goodwin and George Segall for making the facilities of this Service available for this study. Dr. John Jacquez provided important advice and assistance with regard to the model identifiability question. This research is supported by Department of Veterans Affairs intramural Medical Research funds (Program 821).

REFERENCES

1. Hays MT 1988 Thyroid hormone and the gut. Endocr Res **14:**203–224.
2. Kerlin P, Phillips S 1982 Variability of motility of the ileum and jejunum in healthy humans. Gastroenterology **82:**694–700.
3. Caride VJ, Prokop EK, Troncale FJ, et al 1984 Scintigraphic determination of small intestinal transit time: Comparison with the hydrogen breath technique. Gastroenterology **86:**714–720.
4. Hays MT, Hsu L, Kohatsu S. Transport of the thyroid hormones across the feline gut wall. In preparation.
5. Berman ME, Shahn E, Weiss MR 1962 The routine fitting of kinetic data to models: A mathematical formalism for digital computers. Biophys J **2:**275–287.
6. Berman M, Beltz WF, Greif PC, Chabay R, Boston RC 1983 Consam: User's Guide. Department of Health and Human Services, Washington, DC.
7. Hays MT 1991 Application of mathematical modeling technique to human thyroid hormone metabolism. In: Wu S-Y (ed) Thyroid and Hormone Metabolism: Regulation and Clinical Implications. Blackwell Scientific, Cambridge, MA.
8. Hays MT 1968 Absorption of oral thyroxine in man. J Clin Endocrinol Metab **28:**749–756.
9. DiStefano JJ, Jang M, Malone TK, Broutman M 1982 Comprehensive kinetics of triiodothyronine production, distribution, and metabolism in blood and tissue pools of the rat using optimized blood-sampling protocols. Endocrinology **110:**198–213.
10. Jacquez JA 1985 Compartmental Analysis in Biology and Medicine. The University of Michigan Press, Ann Arbor.
11. DiStefano JJ 1980 Design and optimization of tracer experiments in physiology and medicine. Fed Proc **39:**84–90.
12. Stone E, Leiter LA, Lambert JR, Silverberg JDH, Jeejeebhoy KN, Burrow GN 1984 L-Thyroxine absorption in patients with short bowel. J Clin Endocrinol Metab **59:**139–141.
13. Azizi F, Belur R, Albano J 1979 Malabsorption of thyroid hormones after jejunoileal bypass for obesity. Ann Intern Med **90:** 941–942.
14. Topliss DJ, Wright JA, Volpe R 1980 Increased requirement for thyroid hormone after a jejunoileal bypass operation. CMA J **123:**765–766.
15. Bevan JS, Munro JF 1986 Thyroxine malabsorption following intestinal bypass surgery. Int J Obes **10:**245–246.

Address reprint requests to:
Marguerite T. Hays, M.D. (151)
DVA Medical Center
3801 Miranda Avenue
Palo Alto, CA 94304